Annals of Nuclear Medicine Vol. 17, No. 5, 341–350, 2003

# Pathophysiology and diagnosis of hibernating myocardium in patients with post-ischemic heart failure: the contribution of PET

Paolo G. CAMICI and Ornella E. RIMOLDI

*MRC Clinical Sciences Centre and National Heart and Lung Institute, Faculty of Medicine, Imperial College of Science, Technology and Medicine, Hammersmith Hospital, London, United Kingdom*

Identification and treatment of hibernating myocardium (HM) lead to improvement in LV function and prognosis in patients with post-ischemic heart failure. Different techniques are used to diagnose HM: echocardiography, MRI, SPECT and PET and, in patients with moderate LV impairment, their predictive values are similar. There are few data on patients with severe LV dysfunction and heart failure in whom the greatest benefits are apparent after revascularization. Quantification of FDG uptake with PET during hyperinsulinemic euglycemic clamp is accurate in these patients with the greatest mortality risk in whom other techniques may give high false negative rates.

The debate on whether resting myocardial blood flow to HM is reduced or not has stimulated new research on heart failure in patients with coronary artery disease. PET with $H_2{}^{15}O$ or $^{13}NH_3$ has been used for the absolute quantification of regional blood flow in human HM. When HM is properly identified, resting blood flow is not different from that in healthy volunteers although a reduction of ~20% can be demonstrated in a minority of cases. PET studies have shown that the main feature of HM is a severe impairment of coronary vasodilator reserve that improves after revascularization in parallel with LV function. Thus, the pathophysiology of HM is more complex than initially postulated. The recent evidence that repetitive ischemia in patients can be cumulative and lead to more severe and prolonged stunning, lends further support to the hypothesis that, at least initially, stunning and HM are two facets of the same coin.

**Key words:** coronary artery disease, congestive heart failure, positron emission tomography, myocardial blood flow, myocardial metabolism

## BACKGROUND

CONFIRMATION of true myocardial hibernation can only be made retrospectively by an improvement in ventricular function after revascularization. The exact prevalence of myocardial hibernation in patients with coronary artery disease and heart failure has not been established, but preliminary studies suggest that up to half of such patients derive a clinically meaningful improvement in left ventricular function after revascularization.[1–5]

Received April 7, 2003, revision accepted April 7, 2003.

For reprint contact: Paolo G. Camici, M.D., MRC Clinical Sciences Centre, Hammersmith Hospital, Ducane Road, London W12 ONN (UK).

E-mail: paolo.camici@csc.mrc.ac.uk

If surgical revascularization is to be employed with the primary aim of improving ventricular function (i.e., as a treatment for heart failure), rather than for relief of angina, it is clear that hibernating myocardium must be identified accurately. The presence of viable myocardium is a strong predictor of improvement in ventricular function and prognosis after bypass surgery (Figs. 1 and 2).[2,4,6–10] Several different techniques can be used to assess myocardial viability: echocardiography and nuclear magnetic resonance imaging during dobutamine stress, SPECT with $^{201}Tl$ or $^{99m}Tc$-labeled compounds, $^{18}F$-fluorodeoxyglucose (FDG) with PET. These methods probe different aspects of myocyte viability, namely, the presence of inotropic contractile reserve, sarcolemmal integrity, and preserved uptake of exogenous glucose, respectively. In patients with normal to moderate impairment of left

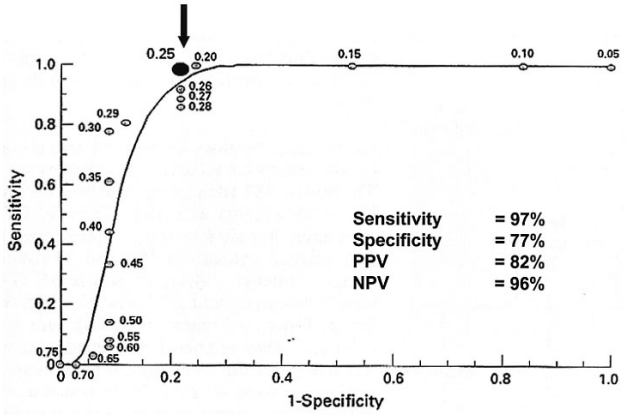


**Fig. 1** PET FDG absolute quantification predicts improvement in segmental left ventricular function. Receiver-operator characteristic (ROC) curve showing sensitivity and specificity in identifying hibernating segments for different values of metabolic rate of glucose (MRG) in $\mu$mol/g/min. The large dot represents the operating point associated with the best compromise between sensitivity and specificity 0.25 $\mu$mol/g/min.

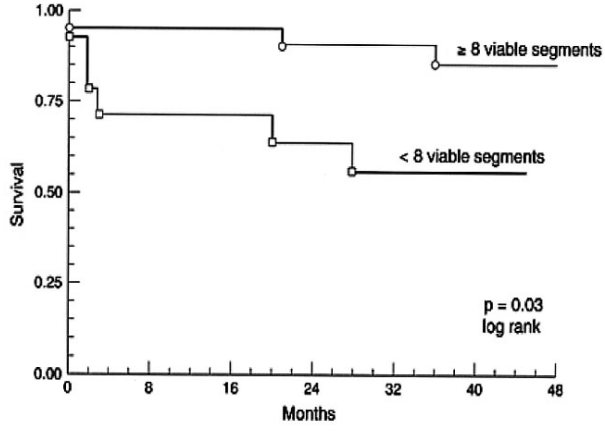


**Fig. 2** Kaplan-Meier curves showing estimated cardiac event free five years survival in patients with ≥8/16 viable segments and <8/16 viable segments.

ventricular function, their predictive value for the identification of hibernating myocardium appears to be similar (positive predictive value, 69% to 83%; negative predictive value, 81% to 90%).[11,12] However, there are few data on patients with severe left ventricular dysfunction and heart failure, and published studies have mostly included patients with limiting angina in whom a decision to revascularize can be made on conventional clinical criteria.

As the greatest clinical benefits accrue to those patients with the most marked ventricular dysfunction,[13] the demonstration of viable myocardium by PET-FDG offers the best predictive accuracy in the patient population with the greatest risk of mortality.[12] Initial studies with PET-FDG and $^{13}$N labeled ammonia ($^{13}NH_3$) as the perfusion tracer, suggested that myocardial ischemia and infarction could be distinguished after an oral load of glucose.[14] Regions of myocardium that exhibited a concordant reduction in $^{13}NH_3$ and FDG uptake (flow-metabolism match) were thought to be predominantly infarcted and to have little prospect of recovery after revascularization, whereas regions in which FDG uptake was relatively preserved, despite a reduction in $^{13}NH_3$ uptake (flow-metabolism mismatch) were considered ischemic, but viable. Viable myocardium is frequently admixed with scar tissue in patients with previous Q wave infarction. The functional recovery after revascularization depends not only on the extent of hibernating myocardium but also on the severity of global left ventricular dysfunction, operative technique, and adequacy of revascularization.[15–17] A clinically meaningful improvement in left ventricular ejection fraction after coronary revascularization has been shown when at least 50% of dysfunctional myocardium is found to be viable.[6,7]

## DIAGNOSIS OF HIBERNATING MYOCARDIUM WITH FDG-PET

The uptake of glucose by the myocardium is dependent on a number of factors such as dietary state, sensitivity to insulin, cardiac workload, sympathetic activity, and severity of ischemia. A number of these factors are clearly interrelated, e.g. insulin resistance is found in patients with coronary artery disease and hypertension as well as type II diabetes and may therefore contribute to the variability in myocardial FDG uptake. The accurate detection of viable myocardium by PET-FDG is therefore dependent on optimization and standardization of the metabolic milieu during the study. It has been suggested that semi-quantitative and quantitative analyses of FDG uptake may enhance the identification of patients with sufficient viable myocardium to benefit from coronary revascularization. However, insulin resistance and the unpredictable response after a standard glucose load, frequently result in poor quality cardiac images. To overcome these potential problems, the hyperinsulinemic euglycemic clamp[18] has been adopted in conjunction with FDG-PET to induce maximum myocardial glucose uptake. In brief, a primed-continuous (40 U/min/m$^2$) infusion of insulin is established and euglycemia maintained by a concomitant infusion of 20% glucose, titrated on the basis of frequent arterialized blood samples.[19,20] Under the near-steady state conditions achieved during the second hour of the insulin clamp, the exogenous infusion of glucose reflects the whole body metabolic use of glucose (assuming suppression of hepatic glucose production). Because the myocardium is amongst the tissues that respond to insulin stimulation by increasing glucose extraction from the blood, this method results in excellent image quality, shows uniform tracer uptake throughout the heart in healthy volunteers, and facilitates comparison between different patients as the data are acquired during

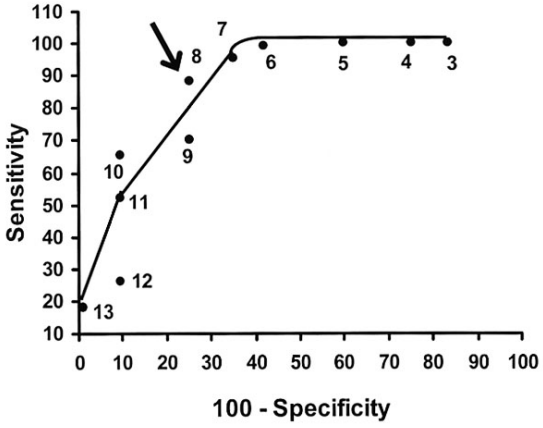


**Fig. 3** ROC curve demonstrating the sensitivity-specificity for the number of PET viable segments required to obtain improvements in LVEF greater than 5 percentage point after coronary artery by-pass graft. The arrow indicates the operator point associated with the best tradeoff between sensitivity (88%) and specificity (75%). The area fitted under the curve is 75%.

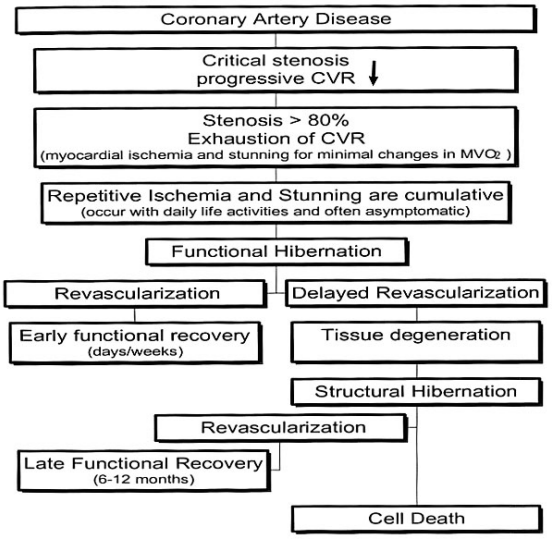


**Fig. 4** Diagram illustrating the interplay of factors contributing to the natural history of hibernating myocardium. CVR = coronary vasodilator reserve.

steady state and under standardized metabolic conditions.[21]

The myocardial uptake of glucose in normally contracting regions of patients with overall ventricular impairment is reduced by some 35% compared with control subjects despite comparable levels of circulating insulin and glucose. Insulin resistance has been shown in the skeletal muscle and adipose tissue of patients with diabetes, hypertension, coronary artery disease, and heart failure, and it remains unclear whether the resistance of the myocardium to insulin as shown by PET-FDG is a distinct phenomenon or part of the whole-body resistance to insulin.[19,21,22] Some of these changes may relate, at least in part, to changes in the lumped constant secondary to myocardial ischemia. This latter cannot, however, be accurately quantified in humans, although the effect is probably limited in regions of myocardium with good ventricular function and blood flow that is well within the normal range at rest.

The precise threshold of glucose uptake by viable but dysfunctional myocardium that identifies those segments that will improve significantly after revascularization in our experience appears to be of the order of 0.25 $\mu$mol/g/min (Fig. 1).[23] However, the results must be considered for each individual patient, and the presence of viable myocardium in 8 or more of the 16 left ventricular segments appears to be associated with significant prognostic benefits (Figs. 2 and 3).[7,24] Although the uptake of glucose (as measured by FDG-PET) is preserved in hibernating myocardial segments, the contractile reserve of the myocytes may be impaired or absent, with myofibrillar loss and changes in myocyte ultrastructure that may explain the false-negative rate of dobutamine stress echocardiography in such patients.[3,4,11,25] In contrast, the preservation of glucose uptake and phosphorylation, including changes in glucose transporter expression,[26] facilitates exogenous glucose use by the ischemic myocyte despite derangement of the contractile apparatus.[27,28] It is likely that early in the natural history of myocardial hibernation, resting contraction is impaired, whereas cellular metabolic function and the capacity to respond to $\beta_1$-adrenergic stimulation are preserved. Later, a more severe form is characterized by reduced basal contractile function and an impaired or absent response to $\beta_1$-adrenergic stimulation; however, glucose uptake is preserved with enhanced glycogen storage and increased expression of glucose transporters. Over time, the metabolic activity of the myocyte decreases further, glucose uptake decreases, and the changes become irreversible with myocyte death (Fig. 4).

## MYOCARDIAL BLOOD FLOW IN HIBERNATING MYOCARDIUM

The debate on whether resting myocardial blood flow (MBF) to hibernating myocardium is reduced or not has attracted a lot of interest and, undoubtedly, has contributed significantly to stimulate new research on heart failure in patients with coronary artery disease (CAD). Although the debate is not over yet, some of the initial paradigms have been proven incorrect while new pathophysiological concepts have emerged.

A number of radionuclide imaging techniques have emerged for the assessment of regional MBF.[29] Their non-invasive nature and the ability to provide simultaneous information on the three different coronary beds have contributed to their widespread application in patients with coronary artery disease. The initial hypothesis that hibernation is due to a down-regulation of myocardial

function secondary to a reduction of resting MBF[30] was supported by a series of studies in which semiquantitative measurements of MBF were performed using different radioactive flow tracers with single photon emission computerized tomography (SPECT) (See ref. 31). Although SPECT enables the assessment of nutritive tissue perfusion, it can only provide images that reflect relative regional radioactivity concentration rather than enabling measurement of absolute MBF (i.e. ml/min/g).[32] The definition of abnormal regional uptake is based on the demonstration of a contrast between two ventricular segments and not an absolute reduction in uptake compared to normal reference values. Therefore, an apparent reduction of radioactivity concentration in one region may reflect higher uptake in the reference region rather than an absolute reduction in the "*defect*" itself.

In addition, the fact that chronically dysfunctional segments are generally thinner than remote normally contracting myocardium will contribute to increase artificially the difference between hibernating and remote myocardium as a consequence of the partial volume effect.[33] This occurs whenever the dimension of the object to be imaged (in our case the thickness of the left ventricular wall) is comparable or smaller than the camera's spatial resolution. Although the detector will accurately record the total activity in the object, it will distribute it over an area larger than the actual size of the object. Hence, the detected radioactivity concentration per unit volume will be less than the actual value.[34]

*PET and absolute myocardial blood flow*

PET overcomes the physical limitations of previously available imaging systems by providing the means for accurate *attenuation correction*, thus enabling accurate quantification of the concentration of radiolabeled tracer in the organ of interest.[35] Photons traveling through a composite medium such as the thorax will be *scattered* by interaction with atomic electrons and undergo change of direction and loss of energy. If a photon is scattered it is 'lost' to the original line of response (the line joining the two PET detectors in coincidence) and the apparent radioactivity measured along that line of response will be less than the truth. This effect is known as *attenuation*. Scatter and attenuation are problems common to all radionuclide imaging techniques and are responsible for most of the artifacts associated with SPECT, particularly when low energy isotopes (e.g. thallium-201) are used. In contrast to SPECT, correction for attenuation is relatively straightforward in PET because of the mechanism of coincidence detection.[34]

As PET technology has advanced and rapid dynamic imaging has become possible, quantification of MBF has been achieved following the development of suitable tracer kinetic models. Oxygen-15 labeled water ($H_2{}^{15}O$)[36–39] and $^{13}NH_3$[40–43] are the tracers most widely used for the quantification of regional MBF with PET. Tracer kinetic models have been successfully validated in animals against the radiolabeled microsphere method for both $H_2{}^{15}O$[36–39] and $^{13}NH_3$.[42,43] Both $H_2{}^{15}O$ and $^{13}NH_3$ have short physical half lives (2 and 10 minutes respectively) which allow repeated measurements of MBF in the same session.[44]

The non-invasive nature of PET and the low radiation dose administered (5–10 times lower than that for SPECT) allows the study of healthy human volunteers. The values of MBF determined using $H_2{}^{15}O$ and $^{13}NH_3$, both at rest and during pharmacologically-induced coronary vasodilatation, are similar[45–50] and PET perfusion studies have highlighted the heterogeneity of both resting and hyperemic MBF in normal human beings.[51] Notwithstanding the inter subjects variability, the short term repeatability of PET assessment of MBF within subjects has been well documented both under resting and hyperemic conditions.[44,52] These data, taken together, have important implications for the interpretation of myocardial perfusion studies in patients with hibernating myocardium.

*The concept of flow per gram of perfusable tissue*

In patients with previous myocardial infarction (a very common finding in patients with hibernating myocardium), the presence and amount of scar tissue within a dysfunctional region may affect the flow estimates made with PET particularly when liquid *deposit tracers* such as $^{13}NH_3$ are used whereas freely diffusible tracers such as $H_2{}^{15}O$ are less affected by this problem.[39,53] $H_2{}^{15}O$ is a metabolically inert and freely diffusible tracer[53] that has a virtually complete myocardial extraction that is independent of both flow rate[54] and myocardial metabolism.[38,55] $^{13}NH_3$ is extracted from blood with an extraction fraction <100%, that is inversely related to the flow rate, and is then trapped in myocardial cells after conversion to $^{13}N$-labeled glutamine, a process mediated by adenosine triphosphate (ATP) and glutamine synthetase.[42,55] Thus, the extent of $^{13}NH_3$ metabolism depends on myocardial ATP stores. When $H_2{}^{15}O$ is used, MBF is estimated from the tracer's washout from the myocardium while in the case of $^{13}NH_3$, MBF is calculated from the tracer's uptake by myocardium. These differences are of little relevance when the measurements of MBF are performed in normal myocardium as proven by the comparable flow estimates obtained with the two tracers in normal human subjects.[45,56] However, if the tissue composition is highly heterogeneous, as in jeopardized myocardium of patients with previous infarction, the flow estimates obtained with these two tracers can show discrepancies. In a highly heterogeneous tissue, the diffusion/extraction and final uptake of $H_2{}^{15}O$ and $^{13}NH_3$ are determined by the flow rates in each tissue compartment, i.e. higher in viable tissue and lower in scar tissue. $^{13}NH_3$ uptake in a given region of interest will reflect the average uptake and hence average flow in this mixture of viable and fibrotic tissue. On the other hand, since the uptake of $H_2{}^{15}O$ in scar tissue is negligible, washout of $H_2{}^{15}O$ will mainly reflect activ-

**Table 1** PET studies of MBF ($^{13}NH_3$) without demonstration of recovery of function at follow up

| Reference | N patients | Previous MI | MBF in remote region (ml/min/g) | MBF in HM region (ml/min/g) | PV correction | Definition of HM |
|---|---|---|---|---|---|---|
| Czernin et al.[78] | 22 | Y recent 21 to 170 hours before | 0.83 ± 0.20 | 0.57 ± 0.20* (range 0.27–0.89) | N | Flow/metabolism mismatch |
| Sambuceti et al.[79] | 33 | N 1 vessel stenosis | 0.77 ± 0.26 | 0.66 ± 0.19* (range 0.43–1.21) | N | Echocardiography |
| Sun et al.[80] | 19 | Y | 0.73 ± 0.23 (range 0.45–1.10) | 0.53 ± 0.33 (range 0.33–0.87) | Y | Flow/metabolism mismatch Echocardiography-low dose dobutamine |
| Brunelli et al.[81] | 15 | Y 30 days before PET | 0.83 ± 0.26 | 0.65 ± 0.27* | N | Echocardiography Dobutamine Flow/metabolism mismatch |
| Marzullo et al.[82] | 14 | Y 1 vessel | 1.00 ± 0.24 | 0.69 ± 14* (45% of dyssynergic segments) 0.42 ± 0.12* (19% of dyssynergic segments) | N | Flow/metabolism mismatch |

* = $p < 0.05$ versus remote region

ity in better perfused segments and the resulting flow can therefore be higher than that obtained with $^{13}NH_3$ in the same region.[21,57,58] Recent refinements of the $H_2{}^{15}O$ technique have permitted incorporation of an estimate of the fraction of tissue (perfusable tissue fraction, PTF) within the volume of interest that is exchanging the freely diffusible tracer into the kinetic model.[59] This technique provides values of flow per gram of perfusable tissue and not per gram of region of interest.[57,58] A further accomplishment is the calculation of the perfusable tissue index (PTI), i.e. the ratio of the perfusable tissue fraction to the total tissue mass (anatomic tissue fraction) in the region of interest.[57] Gerber et al. in a parallel assessment of MBF with $H_2{}^{15}O$ and $^{13}NH_3$ showed that in normal and reversibly dysfunctional myocardium the two techniques yield similar results whereas discordant findings were observed in persistently dysfunctional segments.[60] These latter are characterized by a significant decrease of PTI and the discrepancies between $H_2{}^{15}O$ and $^{13}NH_3$ MBF estimates are smoothed when $H_2{}^{15}O$ MBF is corrected for PTI.[60]

*The partial volume effect*

The loss of systolic wall thickening and presence of scar with wall thinning result in a "partial volume effect" (discussed in more detail previously) that can lead to a 15–25% underestimation of regional radioactivity counts and therefore contribute to the lower MBF computed in these dysfunctional regions. The rectification of the underestimation of myocardial radioactivity due to the partial volume effect and cardiac wall motion is essential for an accurate measure of MBF in cardiac PET studies.[61] However, the correction for "partial volume effect" has not been undertaken in all PET studies in patients with heart failure and hibernating myocardium (see Tables 1–3).[33]

*PET studies of MBF in patients with hibernating myocardium*

The literature can on occasion appear confused, as variable results have been reported in different PET studies.[31,62] There are a number of technical reasons (see above) that affect the various PET studies to different extents and can explain, at least in part, this apparent discrepancy. Moreover, one has to consider the issue of whether flow in hibernating segments should be compared with flow in normally contracting, remote segments in the same patients or with the data obtained in matched normal volunteers.

Therefore, direct comparison of different PET studies must be carefully weighed considering a number of factors: a) demonstration of functional recovery after revascularization, the latter being the definitive criterion to define a dysfunctional segment subtended by a stenotic artery as "hibernating"; b) the characteristics of the tracer and kinetic model used and c) whether appropriate corrections for the calculation of MBF have been applied.

For instance, all the five studies summarized in Table 1 did not include demonstration of functional recovery of dysfunctional myocardium and in most cases correction

**Table 2** PET studies of MBF using $H_2{}^{15}O$ in patients with hibernating myocardium

| Reference | N patients | Previous MI | MBF in remote region (ml/min/g) | MBF in HM region (ml/min/g) | PV correction | Functional recovery assessment |
|---|---|---|---|---|---|---|
| De Silva et al.[57] | 7 | Y acute | 0.97 ± 0.28 | 0.68 ± 0.32* (range 0.46–1.37) | Y | Echocardiography (4 months) |
| Conversano et al.[83] | 17 | Y (11/17) | 0.85 ± 0.36 | 0.65 ± 0.28* (range 0.3–0.25) | N | Echocardiography (2.9 ± 1.1 months) |
| Marinho et al.[21] | 30 | Y (30/30) | 0.92 ± 0.25 | 0.87 ± 0.31 | Y | Radionuclide ventriculography (4–6 months) |
| Mäki et al.[84] | 6 | N | 1.02 ± 0.23 | 0.81 ± 0.27 * | Y | Echocardiography (8 ± 3 months) |
| Mäki et al.[85] | 5 | N | 0.81 ± 0.15 | 0.77 ± 0.18 (range 0.64–1.14) | Y | Echocardiography (8–11 months) |
| Gerber et al.[60] | 16 | Y | 0.83 ± 0.06 | 0.74 ± 0.06 | Y | Echocardiography (7.5 ± 2.1 months) |
| Fath-Ordoubadi et al.[23] | 18 | N 1/24 | 0.89 ± 0.24 | 0.82 ± 0.26 | Y | Echocardiography (4.2 ± 0.5 months) |
| Pagano et al.[77] | 22 | Y | 1.02 ± 0.23 | 1.02 ± 0.24 | Y | Echocardiography (6 months) |

* = $p < 0.05$ versus remote region

**Table 3** PET studies of MBF using $^{13}NH_3$ in patients with hibernating myocardium

| Reference | N patients | Previous MI | MBF in remote region (ml/min/g) | MBF in HM region (ml/min/g) | PV correction | Functional recovery assessment |
|---|---|---|---|---|---|---|
| Vanoverschelde et al.[64] | 26 | N | 0.95 ± 0.27 | 0.77 ± 0.25* | Y | Contrast ventriculography 12/26 (5–8 months) |
| Vanoverschelde et al.[63] | 19 | Y | 0.77 ± 0.18 | 0.82 ± 0.29 | Y | Echocardiography (10 days–2 months–6 months) |
| Gerber et al.[4] | 24 | Y | 0.82 ± 0.22 | 0.84 ± 0.27 | Y | Echocardiography (5 ± 1.9 months) |
| Gerber et al.[60] | 16 | Y | 0.77 ± 0.04 | 0.84 ± 0.08 | Y | Echocardiography (7.5 ± 2.1 months) |
| Grandin et al.[86] | 19 | Y (6/17) | 0.98 ± 0.18 | 0.75 ± 0.20* (range 0.45–1.10) | Y | Contrast ventriculography (6–9 months) |
| Kitsiou et al.[87] | 26 | Not reported | 0.64 ± 0.24 | 0.63 ± 0.27 | N | Radionuclide angiography (10/26) MRI (16/26) (2.5 ± 0.8 months PTCA) (5.8 ± 8.8 months CABG) |
| Maes et al.[28] | 23 | Y (5/23) | 0.64 ± 0.12 0.61 ± 0.13 (range 0.39–0.89) | 0.94 ± 0.11* 0.93 ± 0.11* (range 0.7–1.19) | Y | Radionuclide angiography (3 months) |

* = $p < 0.05$ versus remote region

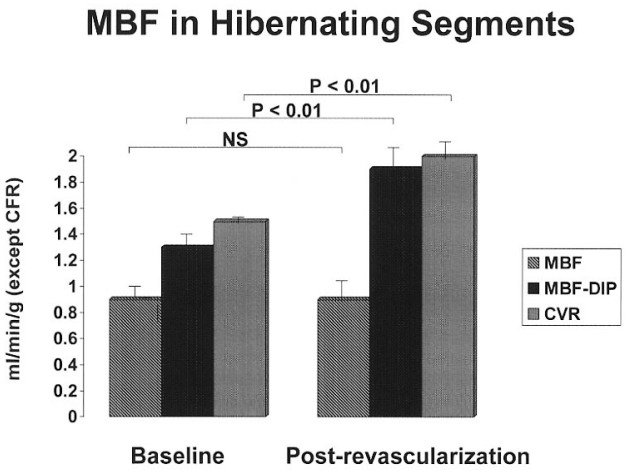


**Fig. 5** Perfusion data on 163 hibernating myocardial segments before (baseline) and after coronary revascularization. MBF = myocardial blood flow; MBF-DIP = post-dipyridamole myocardial blood flow; CVR = coronary vasodilator reserve.

for partial volume was not applied. The demonstration of viability, i.e. flow/metabolism mismatch assessed with $^{13}NH_3$ and FDG and PET was taken as indirect evidence of hibernation. It must be pointed out that the presence of flow/metabolism mismatch is not necessarily associated with functional recovery after revascularization, the latter being mainly dictated by the amount of fibrotic tissue within the region of interest.[27,63] On the other hand, when demonstration of functional recovery after revascularization is used for the definition of hibernation, both $H_2{}^{15}O$ and $^{13}NH_3$ give comparable results. In 9 out of 15 studies reported in Tables 2 and 3, MBF in hibernating segments was not significantly different from MBF in remote, normally contracting myocardium whereas in 6 studies a ~20% lower MBF was found in hibernating segments compared to remote myocardium. Although the paired comparison of flow in dysfunctional and remote areas is statistically more powerful than comparing patients with a normal matched population, the data need to be carefully weighed and regional differences in cardiac workload considered. The difference observed might be explained, at least in part, by a higher MBF in the remote normally contracting regions rather than by an absolute reduction in hibernating segments. The latter would be consistent with the higher oxygen consumption reported in regions remote from segments with severe wall motion abnormalities.[64]

*Coronary flow reserve and hibernation*

The coronary flow reserve is the ratio of MBF during near maximal vasodilatation (pharmacologically-induced) to resting MBF and is an index of the functional significance of coronary stenoses. In patients with coronary artery disease, flow reserve decreases in proportion to the degree of stenosis severity and is abolished (i.e. hyperemic MBF = resting MBF) for stenoses ≥80% of the luminal diameter.[65,66] Under these circumstances, any increase in cardiac workload above baseline conditions cannot be met by an adequate increase in MBF, leading to ischemia. Therefore, in patients with severe coronary artery disease the limited flow reserve leads to the development of myocardial ischemia, which is often asymptomatic[67] even for small increases of oxygen demand such as those associated with ordinary daily activities.[68] Regardless of the blood flow level under baseline conditions, these patients will develop ischemia when oxygen demand is increased (demand ischemia) (Fig. 5). Myocardial ischemia is invariably associated with the development of post-ischemic contractile dysfunction that persists following reperfusion despite the restoration of normal or near-normal coronary blood flow. In the mid seventies this phenomenon, later on known as myocardial stunning,[69] was initially described by Heyndrickx et al.[70] as a sustained, but eventually completely reversible post-ischemic contractile dysfunction in a conscious healthy dog model subjected to a 15-minute coronary occlusion. Two decades later it has been shown that patients with chronic coronary artery disease and absence of contractile dysfunction at rest may also develop myocardial stunning after induction of ischemia with exercise or dobutamine.[71–73] MBF was measured using PET and $H_2{}^{15}O$ in patients with CAD and normal LV function. Global (EF) and regional LV systolic function (SF) were measured using quantitative echocardiography during and after dobutamine-induced ischemia. The results of this study show that EF and SF were reduced 30 minutes after dobutamine, but recovered by 120 minutes. MBF (ml/min/g) to regions with reversible LV dysfunction was normal at baseline and during dysfunction (0.88 and 1.09 respectively, p = NS). In conclusions, in patients with CAD, dobutamine produces prolonged, but reversible LV dysfunction when MBF is normal, thus confirming the occurrence of stunning.[73]

In addition, we have recently demonstrated that in patients with stable exercise-inducible ischemia and normal ventricular function, repeated episodes of ischemia may be cumulative and culminate in more prolonged and severe post ischemic stunning.[74]

Thus, in the long term, intermittent episodes of ischemia followed by stunning might induce regional alterations in the myocytes thus contributing to the development of persistent, but still reversible left ventricular dysfunction.[64,75] Clearly, under these conditions, coronary revascularization by restoring flow reserve could interrupt the vicious circle that has led to chronic ischemic dysfunction.[76,77]

In a recent study Vanoverschelde et al.[63] showed that adequate revascularization is not always sufficient for subsequent complete recovery; successful revascularization was achieved in all patients, but only 19/32 had an improved function at six months. In those patients the extent of recovery was determined by a combination of

several independent factors such as: MBF ($^{13}NH_3$), end-diastolic volume, glucose uptake and the proportion of extracellular matrix.

## CONCLUSIONS

In summary, the measurement of regional myocardial glucose utilization and absolute myocardial blood flow using positron emission tomography has contributed significantly to a better understanding of the pathophysiology of hibernating myocardium in patients with coronary artery disease.

## REFERENCES


1. Bonow RO. The hibernating myocardium: implications for management of congestive heart failure. *Am J Cardiol* 1995; 75 (3): 17A–25A.
2. Eitzman D, et al. Clinical outcome of patients with advanced coronary artery disease after viability studies with positron emission tomography. *J Am Coll Cardiol* 1992; 20 (3): 559–565.
3. Pagano D, et al. Predictive value of dobutamine echocardiography and positron emission tomography in identifying hibernating myocardium in patients with postischaemic heart failure. *Heart* 1998; 79 (3): 281–288.
4. Gerber BL, et al. Myocardial blood flow, glucose uptake, and recruitment of inotropic reserve in chronic left ventricular ischemic dysfunction. Implications for the pathophysiology of chronic myocardial hibernation. *Circulation* 1996; 94 (4): 651–659.
5. Samady H, et al. Failure to improve left ventricular function after coronary revascularization for ischemic cardiomyopathy is not associated with worse outcome. *Circulation* 1999; 100 (12): 1298–1304.
6. vom Dahl J, et al. Relation of regional function, perfusion, and metabolism in patients with advanced coronary artery disease undergoing surgical revascularization. *Circulation* 1994; 90 (5): 2356–2366.
7. Pagano D, et al. Coronary revascularisation for postischaemic heart failure: how myocardial viability affects survival. *Heart* 1999; 82 (6): 684–688.
8. Pagley PR, et al. Improved outcome after coronary bypass surgery in patients with ischemic cardiomyopathy and residual myocardial viability. *Circulation* 1997; 96 (3): 793–800.
9. Dreyfus GD, et al. Myocardial viability assessment in ischemic cardiomyopathy: benefits of coronary revascularization. *Ann Thorac Surg* 1994; 57 (6): 1402–1407; discussion 1407–1408.
10. Di Carli MF, et al. Quantitative relation between myocardial viability and improvement in heart failure symptoms after revascularization in patients with ischemic cardiomyopathy. *Circulation* 1995; 92 (12): 3436–3444.
11. Bonow RO. The hibernating myocardium: identification of viable myocardium in patients with coronary artery disease and chronic left ventricular dysfunction. *Basic Res Cardiol* 1995; 90 (1): 49–51.
12. Bax JJ, et al. Time course of functional recovery of stunned and hibernating segments after surgical revascularization. *Circulation* 2001; 104 (12 Suppl 1): I314–I318.
13. Fath-Ordoubadi F, et al. Coronary revascularization in the treatment of moderate and severe postischemic left ventricular dysfunction. *Am J Cardiol* 1998; 82 (1): 26–31.
14. Tillisch J, et al. Reversibility of cardiac wall-motion abnormalities predicted by positron tomography. *N Engl J Med* 1986; 314 (14): 884–888.
15. Brunken R, et al. Regional perfusion, glucose metabolism, and wall motion in patients with chronic electrocardiographic Q wave infarctions: evidence for persistence of viable tissue in some infarct regions by positron emission tomography. *Circulation* 1986; 73 (5): 951–963.
16. Bax JJ, et al. Accuracy of currently available techniques for prediction of functional recovery after revascularization in patients with left ventricular dysfunction due to chronic coronary artery disease: comparison of pooled data. *J Am Coll Cardiol* 1997; 30 (6): 1451–1460.
17. Armstrong WF, et al. Stress echocardiography: recommendations for performance and interpretation of stress echocardiography. Stress Echocardiography Task Force of the Nomenclature and Standards Committee of the American Society of Echocardiography. *J Am Soc Echocardiogr* 1998; 11 (1): 97–104.
18. DeFronzo RA, Tobin JD, Andres R. Glucose clamp technique: a method for quantifying insulin secretion and resistance. *Am J Physiol* 1979; 237 (3): E214–E223.
19. Paternostro G, et al. Cardiac and skeletal muscle insulin resistance in patients with coronary heart disease. A study with positron emission tomography. *J Clin Invest* 1996; 98 (9): 2094–2099.
20. Paternostro G, et al. Insulin resistance in patients with cardiac hypertrophy. *Cardiovasc Res* 1999; 42 (1): 246–253.
21. Marinho NV, et al. Pathophysiology of chronic left ventricular dysfunction. New insights from the measurement of absolute myocardial blood flow and glucose utilization. *Circulation* 1996; 93 (4): 737–744.
22. Iozzo P, et al. Independent association of type 2 diabetes and coronary artery disease with myocardial insulin resistance. *Diabetes* 2002; 51 (10): 3020–3024.
23. Fath-Ordoubadi F, et al. Efficacy of coronary angioplasty for the treatment of hibernating myocardium. *Heart* 1999; 82 (2): 210–216.
24. Meluzin J, et al. Prognostic value of the amount of dysfunctional but viable myocardium in revascularized patients with coronary artery disease and left ventricular dysfunction. Investigators of this Multicenter Study. *J Am Coll Cardiol* 1998; 32 (4): 912–920.
25. Perrone-Filardi P, et al. Assessment of myocardial viability in patients with chronic coronary artery disease. Rest-4-hour–24-hour $^{201}$Tl tomography versus dobutamine echocardiography. *Circulation* 1996; 94 (11): 2712–2719.
26. Brosius FC 3rd, et al. Increased sarcolemmal glucose transporter abundance in myocardial ischemia. *Am J Cardiol* 1997; 80 (3A): 77A–84A.
27. Depre C, et al. Structural and metabolic correlates of the reversibility of chronic left ventricular ischemic dysfunction in humans. *Am J Physiol* 1995; 268 (3 Pt 2): H1265–H1275.
28. Maes A, et al. Histological alterations in chronically

hypoperfused myocardium. Correlation with PET findings. *Circulation* 1994; 90 (2): 735–745.
29. Dilsizian V, Bonow RO. Current diagnostic techniques of assessing myocardial viability in patients with hibernating and stunned myocardium. *Circulation* 1993; 87: 2070.
30. Rahimtoola SH. A perspective on the three large multicenter randomized clinical trials of coronary bypass surgery for chronic stable angina. *Circulation* 1985; 72 (6 Pt 2): V123–V135.
31. Heusch G. Hibernating myocardium. *Physiol Rev* 1998; 78 (4): 1055–1085.
32. Camici PG, et al. Pathophysiological mechanisms of chronic reversible left ventricular dysfunction due to coronary artery disease (hibernating myocardium). *Circulation* 1997; 96 (9): 3205–3214.
33. Hoffman EJ, Huang SC, Phelps ME. Quantitation in positron emission computed tomography: 1. Effect of object size. *J Comput Assist Tomogr* 1979; 3 (3): 299–308.
34. Camici PG, Rosen SD, Spinks TJ. Positron Emission Tomography, in *Nuclear Medicine in Clinical Diagnosis and Treatment*, Murray IPC, Ell PJ (eds), London; Churchill-Livingstone, 1998: 1353–1368.
35. Hoffman EJ, Phelps ME. Positron emission tomography: principles and quantitation, in *Positron emission tomography and autoradiography: principles and applications for the brain and for the heart*, Phelps ME, Mazziotta J, Schelbert H (eds), New York; Raven Press, 1986: 113–148.
36. Bergmann SR, et al. Noninvasive quantitation of myocardial blood flow in human subjects with oxygen-15-labeled water and positron emission tomography. *J Am Coll Cardiol* 1989; 14 (3): 639–652.
37. Araujo LI, et al. Noninvasive quantification of regional myocardial blood flow in coronary artery disease with oxygen-15-labeled carbon dioxide inhalation and positron emission tomography. *Circulation* 1991; 83 (3): 875–885.
38. Bergmann SR, et al. Quantification of regional myocardial blood flow *in vivo* with $H_2{}^{15}O$. *Circulation* 1984; 70 (4): 724–733.
39. Iida H, et al. Measurement of absolute myocardial blood flow with $H_2{}^{15}O$ and dynamic positron-emission tomography. Strategy for quantification in relation to the partial-volume effect. *Circulation* 1988; 78 (1): 104–115.
40. Schelbert HR, et al. Regional myocardial perfusion assessed with N-13 labeled ammonia and positron emission computerized axial tomography. *Am J Cardiol* 1979; 43 (2): 209–218.
41. Krivokapich J, et al. $^{13}N$ ammonia myocardial imaging at rest and with exercise in normal volunteers. Quantification of absolute myocardial perfusion with dynamic positron emission tomography. *Circulation* 1989; 80 (5): 1328–1337.
42. Bellina CR, et al. Simultaneous *in vitro* and *in vivo* validation of nitrogen-13-ammonia for the assessment of regional myocardial blood flow. *J Nucl Med* 1990; 31 (8): 1335–1343.
43. Hutchins GD, et al. Noninvasive quantification of regional blood flow in the human heart using N-13 ammonia and dynamic positron emission tomographic imaging. *J Am Coll Cardiol* 1990; 15 (5): 1032–1042.
44. Kaufmann PA, et al. Assessment of the reproducibility of baseline and hyperemic myocardial blood flow measurements with $^{15}O$-labeled water and PET. *J Nucl Med* 1999; 40 (11): 1848–1856.
45. Nitzsche EU, et al. Noninvasive quantification of myocardial blood flow in humans. A direct comparison of the [$^{13}N$]ammonia and the [$^{15}O$]water techniques. *Circulation* 1996; 93 (11): 2000–2006.
46. Bol A, et al. Direct comparison of [$^{13}N$]ammonia and [$^{15}O$]water estimates of perfusion with quantification of regional myocardial blood flow by microspheres. *Circulation* 1993; 87 (2): 512–525.
47. Camici PG, et al. The impact of myocardial blood flow quantitation with PET on the understanding of cardiac diseases. *Eur Heart J* 1996; 17 (1): 25–34.
48. Camici PG, Rosen SD. Does positron emission tomography contribute to the management of clinical cardiac problems? *Eur Heart J* 1996; 17 (2): 174–181.
49. Austin RE Jr, et al. Profound spatial heterogeneity of coronary reserve. Discordance between patterns of resting and maximal myocardial blood flow. *Circ Res* 1990; 67 (2): 319–331.
50. Bassingthwaighte JB, King RB, Roger SA. Fractal nature of regional myocardial blood flow heterogeneity. *Circ Res* 1989; 65 (3): 578–590.
51. Czernin J, et al. Influence of age and hemodynamics on myocardial blood flow and flow reserve. *Circulation* 1993; 88 (1): 62–69.
52. Nagamachi S, Czernin J, Kim AS. Reproducibility of measurement of regional resting and hyperemic myocardial blood flow assessed with PET. *J Nucl Med* 1996; 37: 1626–1631.
53. Johnson JA, Cavert HM, Lifson N. Kinetics concerned with distribution of isotopic water in isolated dog heart and skeletal muscle. *Am J Physiol* 1952; 171: 687–693.
54. Yipintsoi T, Bassingthwaighte JB. Circulatory transport of iodoantipyrine and water in the isolated dog heart. *Circ Res* 1970; 27 (3): 461–477.
55. Bergmann SR, et al. The dependence of accumulation of $^{13}NH_3$ by myocardium on metabolic factors and its implications for quantitative assessment of perfusion. *Circulation* 1980; 61 (1): 34–43.
56. Camici PG, Spinks TJ. Advance imaging-PET, in *Challenges in acute coronary syndromes*, de Bono DSB (ed), Oxford; Blackwell Science, 1998: 148–172.
57. de Silva R, et al. Preoperative prediction of the outcome of coronary revascularization using positron emission tomography. *Circulation* 1992; 86 (6): 1738–1742.
58. Lammertsma AA, et al. Measurement of regional myocardial blood flow using $C^{15}O_2$ and positron emission tomography: comparison of tracer models. *Clin Phys Physiol Meas* 1992; 13 (1): 1–20.
59. Iida H, et al. Myocardial tissue fraction—correction for partial volume effects and measure of tissue viability. *J Nucl Med* 1991; 32 (11): 2169–2175.
60. Gerber BL, et al. Nitrogen-13-ammonia and oxygen-15-water estimates of absolute myocardial perfusion in left ventricular ischemic dysfunction. *J Nucl Med* 1998; 39 (10): 1655–1662.
61. Iida H, et al. Myocardial tissue fraction correction for partial volume effects and measure of tissue viability. *J Nucl Med* 1991; 32: 2169–2175.
62. Canty JM Jr, Fallavollita JA. Resting myocardial flow in

hibernating myocardium: validating animal models of human pathophysiology. *Am J Physiol* 1999; 277 (1 Pt 2): H417–H422.
63. Vanoverschelde JL, et al. Time course of functional recovery after coronary artery bypass graft surgery in patients with chronic left ventricular ischemic dysfunction. *Am J Cardiol* 2000; 85 (12): 1432–1439.
64. Vanoverschelde JL, et al. Mechanisms of chronic regional postischemic dysfunction in humans. New insights from the study of noninfarcted collateral-dependent myocardium. *Circulation* 1993; 87 (5): 1513–1523.
65. Uren NG, et al. Relation between myocardial blood flow and the severity of coronary-artery stenosis. *N Engl J Med* 1994; 330 (25): 1782–1788.
66. Di Carli M, et al. Relation among stenosis severity, myocardial blood flow, and flow reserve in patients with coronary artery disease. *Circulation* 1995; 91 (7): 1944–1951.
67. Rosen SD, et al. Silent ischemia as a central problem: regional brain activation compared in silent and painful myocardial ischemia. *Ann Intern Med* 1996; 124 (11): 939–949.
68. Deanfield JE, et al. Myocardial ischaemia during daily life in patients with stable angina: its relation to symptoms and heart rate changes. *Lancet* 1983; 2 (8353): 753–758.
69. Braunwald E, Kloner RA. The stunned myocardium: prolonged, postischemic ventricular dysfunction. *Circulation* 1982; 66 (6): 1146–1149.
70. Heyndrickx GR, et al. Regional myocardial functional and electrophysiological alterations after brief coronary artery occlusion in conscious dogs. *J Clin Invest* 1975: 56 (4): 978–985.
71. Ambrosio G, et al. Prolonged impairment of regional contractile function after resolution of exercise-induced angina. Evidence of myocardial stunning in patients with coronary artery disease. *Circulation* 1996; 94 (10): 2455–2464.
72. Barnes E, et al. Prolonged left ventricular dysfunction occurs in patients with coronary artery disease after both dobutamine and exercise induced myocardial ischaemia. *Heart* 2000; 83 (3): 283–289.
73. Barnes E, et al. Absolute blood flow and oxygen consumption in stunned myocardium in patients with coronary artery disease. *J Am Coll Cardiol* 2002; 39 (3): 420–427.
74. Barnes E, et al. Effect of repeated episodes of reversible myocardial ischemia on myocardial blood flow and function in humans. *Am J Physiol Heart Circ Physiol* 2002; 282 (5): H1603–H1608.
75. Ross J Jr. Myocardial perfusion-contraction matching. Implications for coronary heart disease and hibernation. *Circulation* 1991; 83 (3): 1076–1083.
76. Pagano D, et al. Effects of coronary revascularisation on myocardial blood flow and coronary vasodilator reserve in hibernating myocardium. *Heart* 2001; 85 (2): 208–212.
77. Pagano D, et al. Hibernating myocardium: morphological correlates of inotropic stimulation and glucose uptake. *Heart* 2000; 83 (4): 456–461.
78. Czernin J, et al. Regional blood flow, oxidative metabolism, and glucose utilization in patients with recent myocardial infarction. *Circulation* 1993; 88 (3): 884–895.
79. Sambuceti G, et al. Regional myocardial blood flow in stable angina pectoris associated with isolated significant narrowing of either the left anterior descending or left circumflex coronary artery. *Am J Cardiol* 1993; 72 (14): 990–994.
80. Sun KT, et al. Effects of dobutamine stimulation on myocardial blood flow, glucose metabolism, and wall motion in normal and dysfunctional myocardium. *Circulation* 1996; 94 (12): 3146–3154.
81. Brunelli C, et al. Improvement of hibernation in the clinical setting. *J Mol Cell Cardiol* 1996; 28 (12): 2415–2418.
82. Marzullo P, et al. Residual coronary reserve identifies segmental viability in patients with wall motion abnormalities. *J Am Coll Cardiol* 1995; 26 (2): 342–350.
83. Conversano A, et al. Delineation of myocardial stunning and hibernation by positron emission tomography in advanced coronary artery disease. *Am Heart J* 1996; 131 (3): 440–450.
84. Mäki M, et al. Glucose uptake in the chronically dysfunctional but viable myocardium. *Circulation* 1996; 93 (9): 1658–1666.
85. Mäki MT, et al. Fatty acid uptake is preserved in chronically dysfunctional but viable myocardium. *Am J Physiol* 1997; 273 (5 Pt 2): H2473–H2480.
86. Grandin C, et al. Delineation of myocardial viability with PET. *J Nucl Med* 1995; 36 (9): 1543–1552.
87. Kitsiou AN, et al. $^{13}$N-ammonia myocardial blood flow and uptake: relation to functional outcome of asynergic regions after revascularization. *J Am Coll Cardiol* 1999; 33 (3): 678–686.